Microtubule-associated Protein 2 within Axons of Spinal Motor Neurons: Associations with Microtubules and Neurofilaments in Normal and β,β′-Iminodipropionitrile-treated Axons

SOZOS CH. PAPASOZOMENOS,* LESTER I. BINDER, PATRICK K. BENDER, and MICHAEL R. PAYNE

*Division of Neuropathology, Department of Pathology; and Department of Biology, University of Virginia School of Medicine, Charlottesville 22908. Dr. Papasozomenos' present address is Department of Pathology and Laboratory Medicine, Medical School, University of Texas Health Science Center at Houston, Texas 77225.

ABSTRACT We have examined the distribution of microtubule-associated protein 2 (MAP2) in the lumbar segment of spinal cord, ventral and dorsal roots, and dorsal root ganglia of control and β,β′-iminodipropionitrile-treated rats. The peroxidase-antiperoxidase technique was used for light and electron microscopic immunohistochemical studies with two monoclonal antibodies directed against different epitopes of Chinese hamster brain MAP2, designated AP9 and AP13. MAP2 immunoreactivity was present in axons of spinal motor neurons, but was not detected in axons of white matter tracts of spinal cord and in the majority of axons of the dorsal root. A gradient of staining intensity among dendrites, cell bodies, and axons of spinal motor neurons was present, with dendrites staining most intensely and axons the least. While dendrites and cell bodies of all neurons in the spinal cord were intensely positive, neurons of the dorsal root ganglia were variably stained. The axons of labeled dorsal root ganglion cells were intensely labeled up to their bifurcation; beyond this point, while only occasional central processes in dorsal roots were weakly stained, the majority of peripheral processes in spinal nerves were positive.

β,β′-Iminodipropionitrile produced segregation of microtubules and membranous organelles from neurofilaments in the peripheral nervous system portion and accumulation of neurofilaments in the central nervous system portion of spinal motor axons. While both anti-MAP2 hybridoma antibodies co-localized with microtubules in the central nervous system portion, only one co-localized with microtubules in the peripheral nervous system portion of spinal motor axons, while the other antibody co-localized with neurofilaments and did not stain the central region of the axon which contained microtubules. These findings suggest that (a) MAP2 is present in axons of spinal motor neurons, albeit in a lower concentration or in a different form than is present in dendrites, and (*b*) the MAP2 in axons interacts with both microtubules and neurofilaments.

Numerous polypeptides co-purify with the microtubule protein tubulin through repetitive cycles of temperature-dependent assembly and disassembly. During this process, those that maintain a constant stoichiometry to tubulin have been termed microtubule-associated proteins (MAPs)[1] (1, 2). The most abundant MAP in neural tissues is a heat-stable, high molecular weight phosphoprotein (M_r ~ 300,000) termed MAP2 (see reference 3 for a review). MAP2 stimulates tubulin

[1] *Abbreviations used in this paper:* CNS, central nervous system; IDPN, β,β′-iminodipropionitrile; MAP, microtubule-associated protein; PEG, polyethylene glycol; PNS, peripheral nervous system.

THE JOURNAL OF CELL BIOLOGY · VOLUME 100 JANUARY 1985 74-85

assembly in vitro, binding periodically along the length of the microtubule and thus stabilizing the formed polymer (1). The filamentous projections, characteristic of MAP2 binding to the microtubule wall, are reminiscent of the side-arms observed in situ, which seem to connect microtubules to membranous organelles (4–9) and to other cytoskeletal structures such as neurofilaments (8–10). Indeed, MAP2 has been shown to co-localize with intermediate filaments in certain cultured brain cells (11). In vitro experiments have demonstrated that neurofilaments are frequent contaminants of bovine brain microtubule preparations and one of the proteins associated with these cytoskeletal structures is MAP2 (12). It has also been shown that MAP2 produces a 20-fold increase in the viscosity of an ATP-induced complex between microtubules and neurofilaments (13). Furthermore, under certain conditions, MAP2 can be competed off from microtubule preparations in vitro by the addition of neurofilaments (14). In addition to its interaction with microtubules and neurofilaments in vitro, MAP2 also binds to actin filaments, causing gelation and bundling of the actin filaments (15–18). Therefore, even though MAP2 is defined as a microtubule-associated protein based on its tubulin binding capacity in vitro, its in vivo association(s) in the various cell types of neural tissues and different cell compartments of individual neurons remain unclear.

Biochemical and immunocytochemical studies have demonstrated that MAP2 is most abundant, but not exclusively restricted to neurons (19–24). Furthermore, immunohistochemical studies have shown that in neurons MAP2 is preferentially distributed in dendrites and cell bodies and it is undetectable in axons (25–28). In addition, axonal transport experiments, performed in the guinea pig optic system, have reproducibly failed to detect transport of any proteins comigrating with MAP2 on SDS-polyacrylamide gels (29). By contrast, a recent report has shown MAP2 immunoreactivity in certain axons within the central nervous system (CNS) (30). Moreover, data have been obtained from biochemical studies on taxol-stabilized microtubules assembled from extracts of bovine cortex (gray matter) and corpus callosum (white matter). These results have shown that, although the MAP2 to tubulin ratio is five times lower in the white matter microtubule preparations than in those obtained from gray matter, significant amounts of MAP2 exist in either the axons or glia of white matter (31). Due to these seemingly conflicting reports, the presence or absence of MAP2 in, at least, certain groups of axons remains unresolved.

To further investigate the cellular and subcellular localization of MAP2 and its possible role in microtubule-neurofilament interactions, we have examined its distribution in control and β,β'-iminodipropionitrile (IDPN)-treated axons. Administration of IDPN, a synthetic neurotoxic compound, to rats selectively and severely impairs the axonal transport of neurofilament proteins, but causes no impairment of the transport of tubulin and actin (32, 33). Also the fast anterograde and retrograde transports, which carry membranous organelles, remain relatively normal (32, 34). This impediment to the transport of neurofilament proteins results in an accumulation of neurofilaments in the CNS portion of the spinal motor neurons (35, 36), beginning at the CNS-peripheral nervous system (PNS) junction and proceeding towards the cell body (33). In the PNS portion of these motor axons, contemporaneously with the cessation of transport of neurofilament proteins, IDPN produces a reorganization of the axoplasmic organelles resulting in segregation of neurofilaments to the cortical axoplasm, and of microtubules, mitochondria, and a large portion of smooth endoplasmic reticulum to the central region of the axon (37–39).

This highly reproducible segregation of two of the major filamentous elements of the cytoskeleton provides an excellent model system in which to study the subcellular distribution of the accessory proteins known to associate with microtubules in vitro and their role in axonal transport. Using this "IDPN model" we have examined the localization of MAP2 within spinal motor axons before and after IDPN administration. We have utilized two monoclonal antibodies directed against different epitopes of MAP2, one monoclonal antibody against β-tubulin, an affinity-purified polyclonal antibody to α- and β-tubulin, and an antiserum against the 68,000-dalton subunit of neurofilaments. Using the peroxidase-antiperoxi-

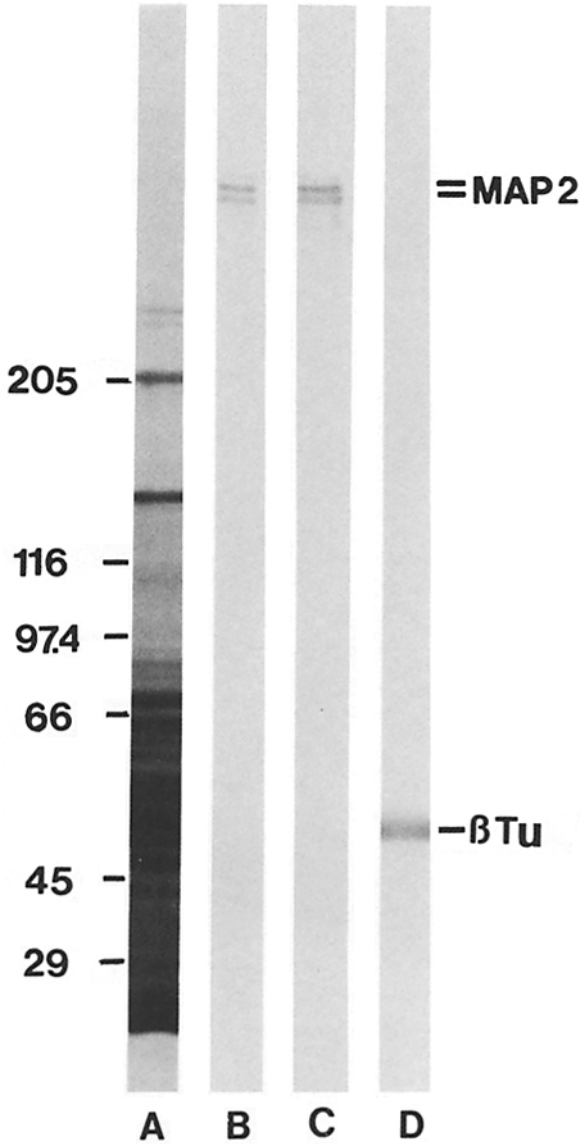

FIGURE 1 Immunoblots of an SDS extract of rat spinal cord, stained with the monoclonal antibodies against MAP2 (AP13 in lane *B* and AP9 in lane *C*) and β-tubulin (lane *D*), using the peroxidase-antiperoxidase technique. Amido black staining was used for protein visualization (lane *A*). The positions of molecular weight standards are marked on the left, while the positions of MAP2 and β-tubulin (βTu) standards are indicated on the right.

dase technique for both light and electron microscopic immunohistochemistry, we demonstrate that (*a*) both antibodies to MAP2 stain the axons of spinal motor neurons and, (*b*) in IDPN-treated rats, both antibodies to MAP2 co-localize with microtubules in the CNS portion but, in the PNS portion of spinal motor axons, one anti-MAP2 antibody localizes with neurofilaments while the other continues to localize with microtubules. Part of this work has appeared in abstract form (40).

MATERIALS AND METHODS

Antibodies: Preparation and characterization of monoclonal antibodies against Chinese hamster brain MAP2, designated AP9 and AP13, and β-tubulin, designated Tu9B, and of rabbit affinity-purified polyclonal antibodies to bovine brain α- and β-tubulin have been described in detail (30, 41, 42). For the present study, the specificities of the monoclonal antibodies to MAP2 and β-tubulin were tested on nitrocellulose immunoblots of homogenates of rat spinal cord and are shown in Fig. 1. Immunoblots were accomplished using SDS-urea polyacrylamide gels (43, 44) which were transferred to nitrocellulose (45), and the antigens observed using the peroxidase-antiperoxidase technique (46, 47).

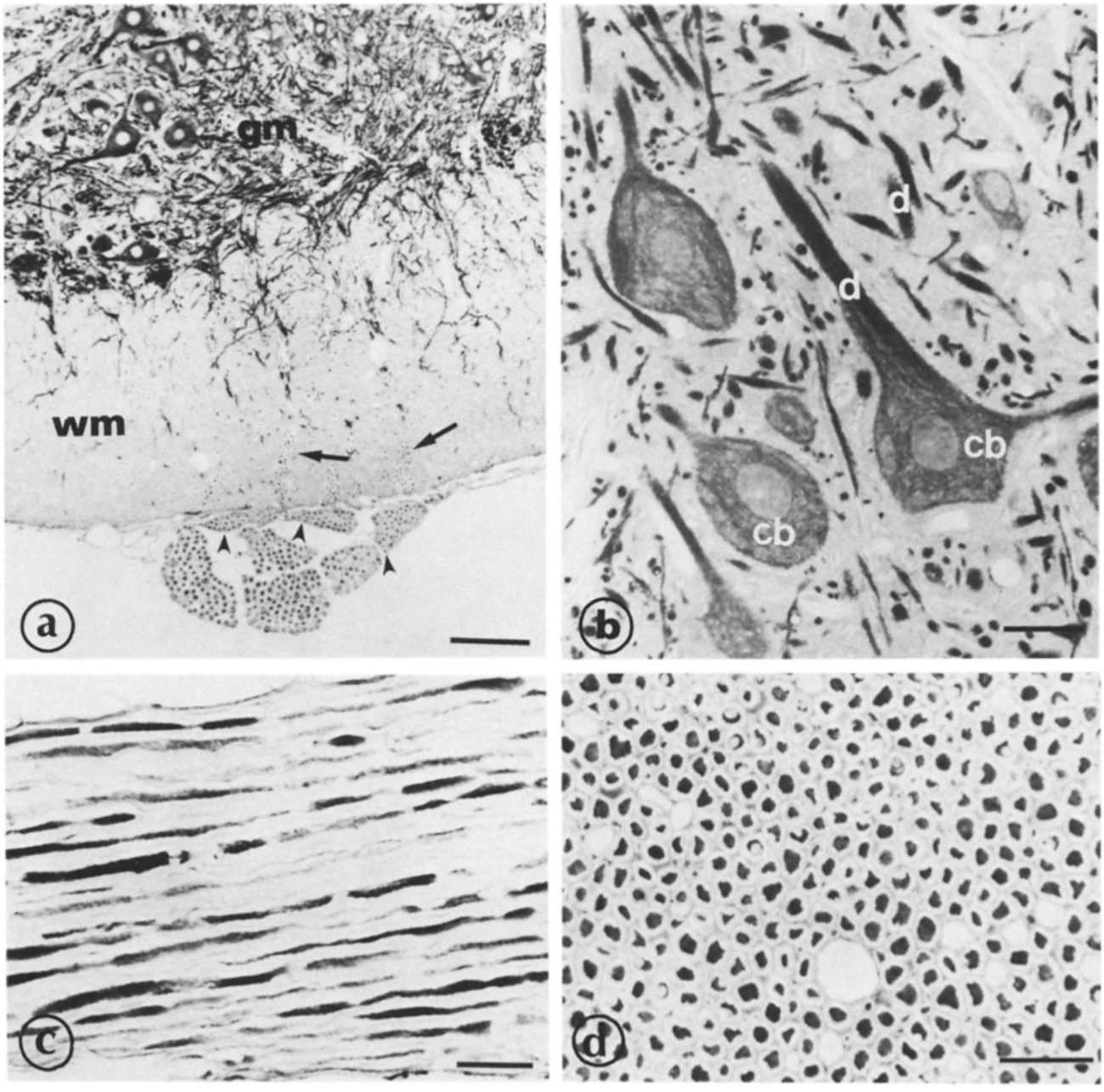

FIGURE 2 Sections from control rat immunostained with AP9 (*a* and *c*) and Ap13 (*b* and *d*). (*a*) Paraffin-embedded cross section of spinal cord and ventral root. *gm*, gray matter; *wm*, white matter. Arrowheads and arrows point to the CNS-PNS junction and CNS portion of motor axons, respectively. Dendrites, cell bodies and axons of motor neurons are strongly stained. AP9 (1.5 μg/ml). Bar, 100 μm. × 125. (*b*) Epon-embedded section of gray matter of spinal cord. The cell bodies (*cb*) of motor neurons show patchy positivity and the dendrites (*d*) are intensely stained. AP13 (39 μg/ml). Bar, 25 μm. × 500. (*c* and *d*) PEG-embedded, longitudinal (c) and cross (*d*) sections of ventral roots. Axons are strongly positive. Section (c) was kept floating in tissue culture well and section (*d*) was mounted on glass slide during immunostaining. (c) AP9 (0.370 μg/ml). (*d*) AP13 (3.9 μg/ml). Bars, 30 μm. (c) × 400. (*d*) × 500.

Total protein transferred from the acrylamide gel to the nitrocellulose was visualized with amido black staining (45). As has been shown (48), AP9 and AP13 are directed against different epitopes on the MAP2 molecule. All three hybridoma antibodies are IgG_1 and their immunoglobulin concentrations prior to dilution (determined as has been described elsewhere [30]) were AP9 0.37 mg/ml; AP13 0.39 mg/ml; Tu9B 0.39 mg/ml. For immunohistochemistry, the antibodies to MAP2 and β-tubulin were used as hybridoma culture supernatants at dilutions of 1:100–1:1,000.

The polyclonal antibody to α- and β- tubulin was used at a concentration of 10 μg/ml and its specificity has been described (42). The characterization of rabbit antiserum against the 68,000-dalton subunit of rat neurofilaments (a gift from Dr. P. Gambetti, Div. of Neuropathology, Institute of Pathology, Case Western Reserve University) has been reported (49) and was used at dilutions of 1:750–1:2,000.

Preadsorption of anti-MAP2 antibodies was performed using purified, heat-stable bovine brain MAP2 attached to an Affi-Gel 10 matrix (Bio-Rad, Richmond, CA). A 10 times concentrated hybridoma culture supernatant was loaded onto the resulting column and the "flow through" was collected. The protein concentration of the "flow through" peak was adjusted to that in the column load. The absence of mouse IgG was determined by double immunodiffusion against a rabbit antimouse IgG polyclonal antiserum.

IDPN Administration: Male Sprague-Dawley rats weighing 200–250 g were given 2 mg/g body weight of IDPN (Eastman Kodak, Rochester, NY), divided into four equal doses and given every 3 d by intraperitoneal injection. IDPN was diluted 1:5 in saline and the pH adjusted to 7.4 with hydrochloric acid. Controls received similar injection of saline.

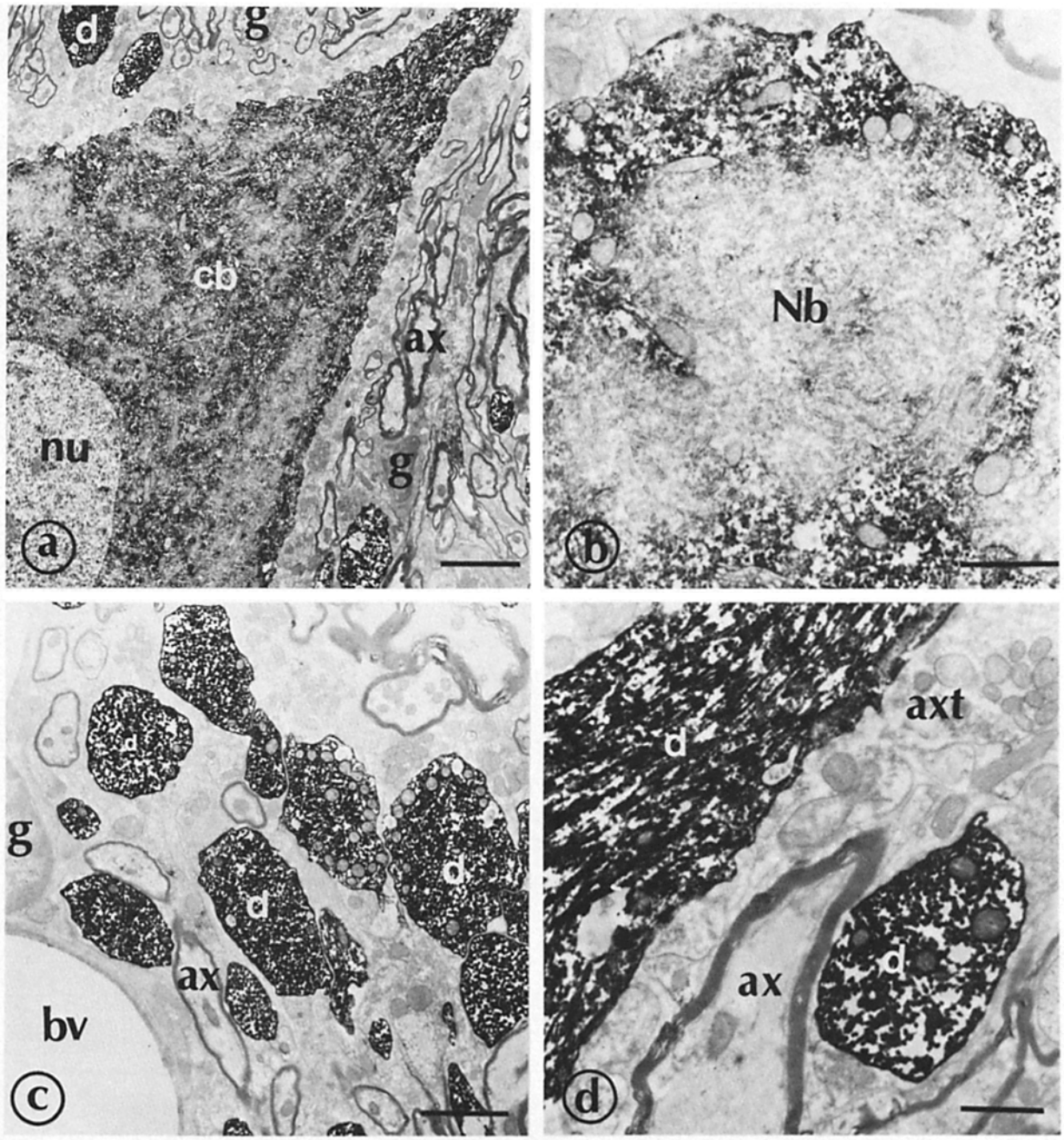

FIGURE 3 Electron micrographs of vibratome sections of lumbar region of spinal cord of a control rat, immunostained with AP13 (0.78 μg/ml). While microtubules in dendrites (*d*) and cell bodies (*cb*) of motor neurons are intensely stained, nearby myelinated axons (*ax*) and axonal terminals (*axt*) are negative. In cell bodies of motor neurons, staining is present in domains of microtubules and mitochondria and is almost absent from domains of Nissl bodies (*Nb*), as is shown in *a* and *b*. Neuronal nuclei (*nu*), glial cells (*g*) and blood vessel walls (*bv*) are negative. Bars: (*b* and *d*) 1 μm, (c) 2 μm, (a) 4 μm. (*a*) × 3,120; (*b*) × 15,200; (*c*) × 6,760; (*d*) × 12,825.

Immunohistochemistry: Control and IDPN-treated rats were sacrificed 2 and 4 d, 1–4, and 6 wk after the fourth injection. Under Nembutal anesthesia, the animals were perfused transcardially with a brief wash of phosphate-buffered saline followed by 800 ml of a mixture of 4% paraformaldehyde and 0.25% glutaraldehyde, in 120 mM sodium potassium phosphate buffer (pH 7.4) at 37°C. Tissue samples were further fixed in 4% paraformaldehyde at 4°C for either another one hour for light microscopy or overnight for light and electron microscopy. Tissue samples, were taken from the lumbar (L) segment of spinal cord, the L_5 ventral and dorsal roots and the L_3, L_4, and L_5 dorsal root ganglia, the sciatic and optic nerves and from several other areas of

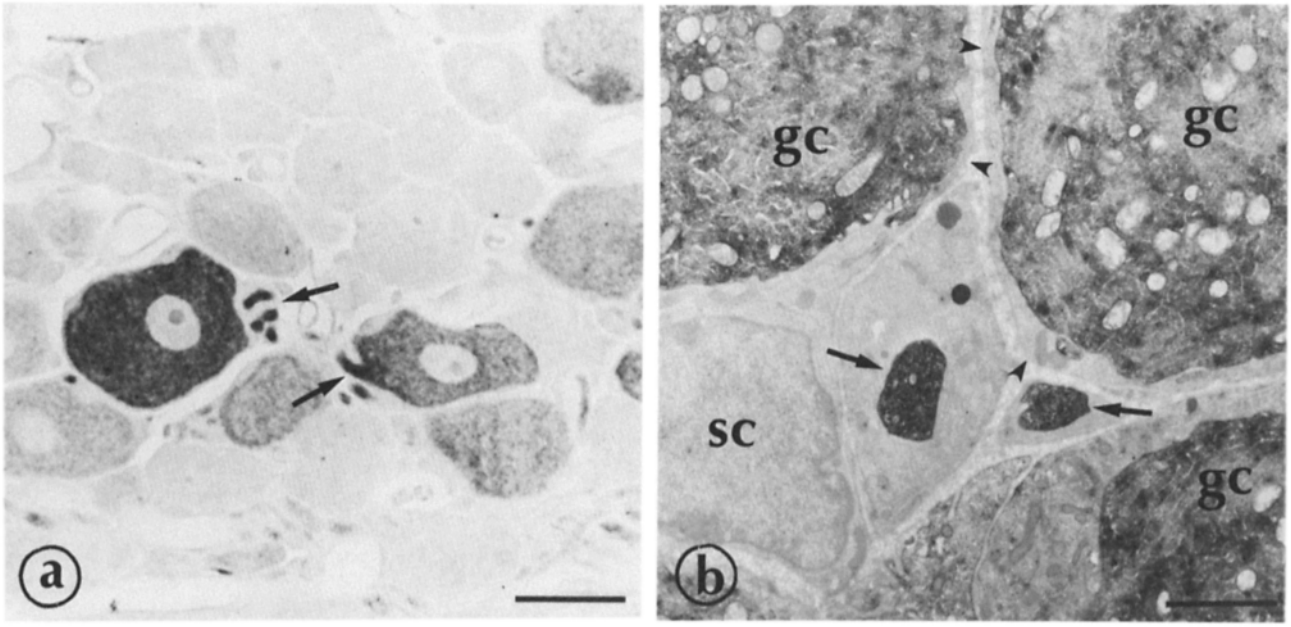

FIGURE 4 L_5 dorsal root ganglia immunostained with AP9. (*a*) Light micrograph of an Epon-embedded section. Intensely stained, negative, and ganglion cells with intermediate staining intensity are present. Arrows point to strongly labeled axons. AP9, 0.37 μg/ml. Bar, 30 μm. × 500. (*b*) Electron micrograph of a vibratome section. Three ganglion cells (*gc*) show patchy cytoplasmic immunoreactivity and two axons (arrows) are intensely stained. Satellite cells (*sc*), which surround ganglion cells, are negative (arrowheads). AP9, 0.74 μg/ml. Bar, 2 μm. × 7,500.

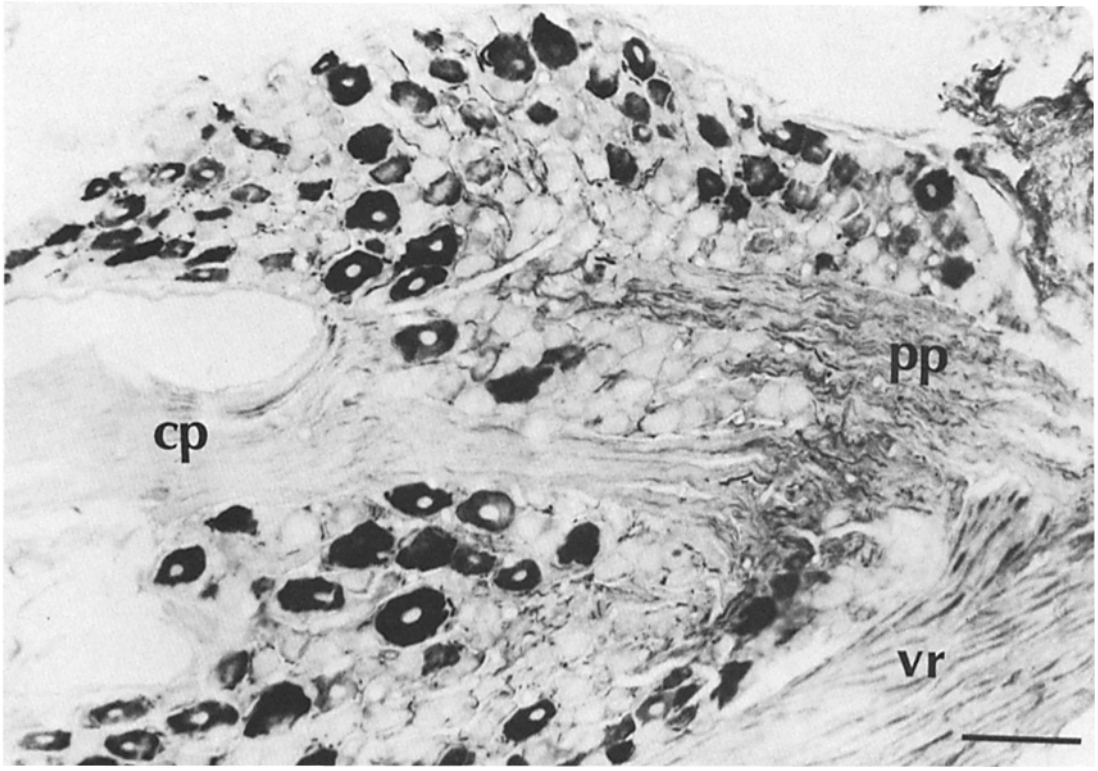

FIGURE 5 Parrafin-embedded section of a dorsal root ganglion and attached ventral root immunostained with AP9 (1.5 μg/ml). Groups of ganglion cells with various degrees of staining intensity are seen. Note the difference between the positive peripheral processes (*pp*), which together with the stained motor axons of ventral root (*vr*) form the spinal nerve, and the negative central processes (*cp*), which constitute the dorsal root. Bar, 100 μm. × 160.

CNS and PNS. They were either dehydrated in alcohol and embedded in Epon, polyethylene glycol (PEG) and paraffin, or sections were cut on a vibratome without prior embedding. PEG-embedding was done in a mixture of 4 parts of 1,000-mol wt PEG to 1 part 3,350-mol wt PEG (Sigma Chemical Co., St. Louis, MO) (50). Light microscopic immunostaining was performed on 3-, 4-, and 6-μm thick sections cut from Epon-, PEG-, and paraffin-embedded tissues, respectively. PEG-embedded sections were mounted on poly-L-lysine-coated glass slides (51). Epon-embedded sections were treated with sodium methoxide to remove the Epon (52) before immunostaining. For electron microscopic immunostaining, 30- or 40-μm thick vibratome or 6-μm thick PEG-embedded sections were used.

The peroxidase-antiperoxidase technique (46, 47) was used for immunostaining. Sections mounted on glass slides or free-floating sections were immunostained by incubating with (*a*) 10% normal goat (Miles Laboratories, Elkhart, IN) or rabbit (Sternberger-Meyer, Jarrettsville, MD) serum, depending on the species of the secondary antibody, to reduce nonspecific staining; (*b*) primary antibody, for 18–36 h at 4°C; (*c*) goat anti-rabbit IgG, diluted 1:50 (Cappel Laboratories, West Chester, PA), or rabbit anti-mouse IgG, diluted 1:40 (Sternberger-Meyer, Jarrettsville, MD); (*d*) rabbit peroxidase-antiperoxidase, diluted 1:200 (Cappel Laboratories, West Chester, PA), or mouse peroxidase-antiperoxidase prepared from monoclonal antibody, diluted 1:150 (Sternberger-Meyer, Jarrettsville, MD); and (*e*) 0.075% diaminobenzidine tetrahydrochloride and 0.015% hydrogen peroxide in 50 mM Tris-HCl, 10 mM imidazole, pH 7.6, for 2–5 min. Incubation times for steps (*a*), (*c*), and (*d*) were 30 min for sections 6 μm thick or less and 90 min for vibratome sections. Dilutions of all antibodies and washings between steps (*b*) and (*c*), and between (*c*) and (*d*) were done with 1% normal goat or rabbit serum in 50 mM Tris-HCl, 0.15 M sodium chloride, pH 7.6. Specificity of staining was determined by absorbing the primary antibodies with a molar excess of the specific antigen and by incubating with nonimmune, or 1% normal goat or rabbit sera in 50 mM Tris-HCl, 0.15 M sodium chloride, pH 7.6.

Following immunostaining, sections for electron microscopy were osmicated in 1% OsO_4 for 30 min, dehydrated in graded alcohols, passed through propylene oxide, and flat-embedded in Epon according to standard procedures. Ultrathin sections were picked up on uncoated grids and viewed without prior staining with heavy metals.

RESULTS

Localization of MAP2 Immunoreactivity in Control Rats

The localizations of two anti-MAP2 antibodies AP9, and AP13, were studied at the light and electron microscopic levels in the lumbar region of spinal cord and ventral roots and in the dorsal root ganglia and dorsal roots.

SPINAL CORD AND VENTRAL ROOTS: In the spinal cord, both AP9 and AP13 intensely stained dendrites and cell bodies of all neurons. A patchy reaction pattern was obtained in cell bodies of motor neurons and no immunoreactivity was present in nuclei (Figs. 2,*a* and *b*, and 3). In addition, both antibodies strongly stained the CNS and PNS (ventral root) portion of motor axons (Fig. 2, *a*, *c*, and *d*). However, a gradient of staining intensity was present among dendrites, neuronal cell bodies and axons of motor neurons, with dendrites staining most intensely and axons the least. In embedded tissues, while both AP9 and AP13 stained axons of spinal motor neurons rather strongly, axons in the white matter tracts of spinal cord were negative (Figs. 2*a* and 10*b*). In vibratome sections, which were immunostained without prior dehydration and embedding, AP9, but not AP13, occasionally stained axons in the white matter, but the reaction was too weak and inconsistent to be reliably interpreted. In general, with the same antibody concentration, AP9 produced a more intense staining of axons than AP13.

DORSAL ROOT GANGLIA AND DORSAL ROOTS: In dorsal root ganglia, a mosaic staining pattern prevailed. Neurons with intense cytoplasmic staining were intermixed with negative neurons and neurons with intermediate intensity of staining (Figs. 4 and 5). While most of the intensely stained neurons were large and the unlabeled were small, several large neurons were negative and several small neurons were strongly positive. The pseudounipolar, axonal process of labeled ganglion cells was intensely stained up to its bifurcation (Fig. 4), and, in general, the staining of the axonal process was stronger than that of the cell bodies. Beyond the bifurcation point, while positive immunoreaction was observed in the peripheral processes, which project into the spinal nerve, no staining was present in the central processes, which constitute the dorsal root (Figs. 5 and 6). However, in a few experiments, there was weak staining in occasional, relatively large axons of dorsal root. Differential staining of dorsal root ganglion cells was also obtained with the antibody to β-tubulin and the antiserum to 68,000-dalton subunit of neurofilaments, but with these antibodies, if the cell bodies were labeled, intense immunoreactivity was present in both their central and peripheral processes (data not shown).

Electron microscopic immunohistochemistry confirmed and extended the light microscopic findings (Figs. 3, 4*b*, and 9*a*). In cell bodies of motor neurons, domains of Nissl bodies remained largely unstained, while regions occupied mostly by microtubules and mitochondria were strongly positive (Fig. 3,*a* and *b*). Thus, the patchy pattern of immunoreactivity in neuronal cell bodies seen with light microscopy (Fig. 2*b*) is largely due to lack of immunoreactivity in Nissl bodies. A similar, but less pronounced, staining pattern was also observed in dorsal root ganglion cells. The staining intensity was further increased in dendrites of spinal neurons and in the axonal processes of labeled dorsal root ganglion cells (Figs. 3, *a*, *c*, and *d*, and 4). In these neuronal processes and in axons of spinal motor neurons (Fig. 9*a*) both AP9 and AP13 decorated microtubules in cross and longitudinal sections. Mitochondria were negative. In contrast to the presence of intense immunoreactivity in dendrites and neuronal cell bodies, nearby, apparently nonmotor, myelinated axons and axonal

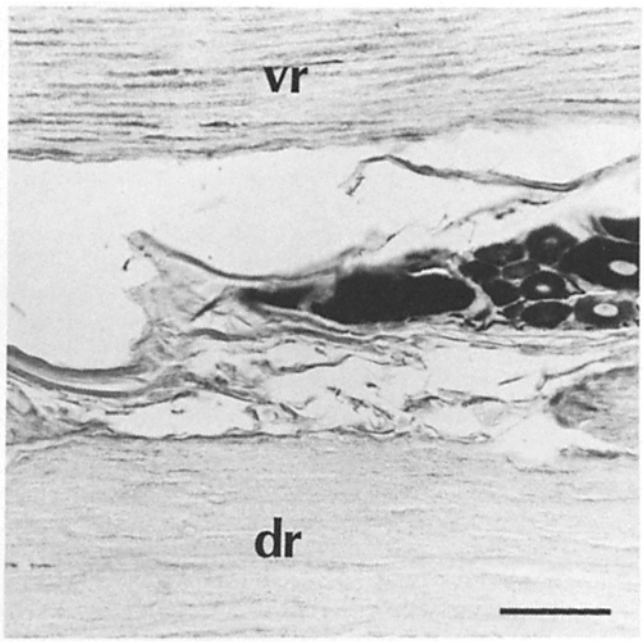

FIGURE 6 A paraffin-embedded longitudinal section of the L_5 dorsal root ganglion with its dorsal root (*dr*) and attached ventral root (*vr*), immunostained with AP9 (1.5 μg/ml). While axons of the ventral root are positive, those of the dorsal root are negative. Bar, 60 μm. × 250.

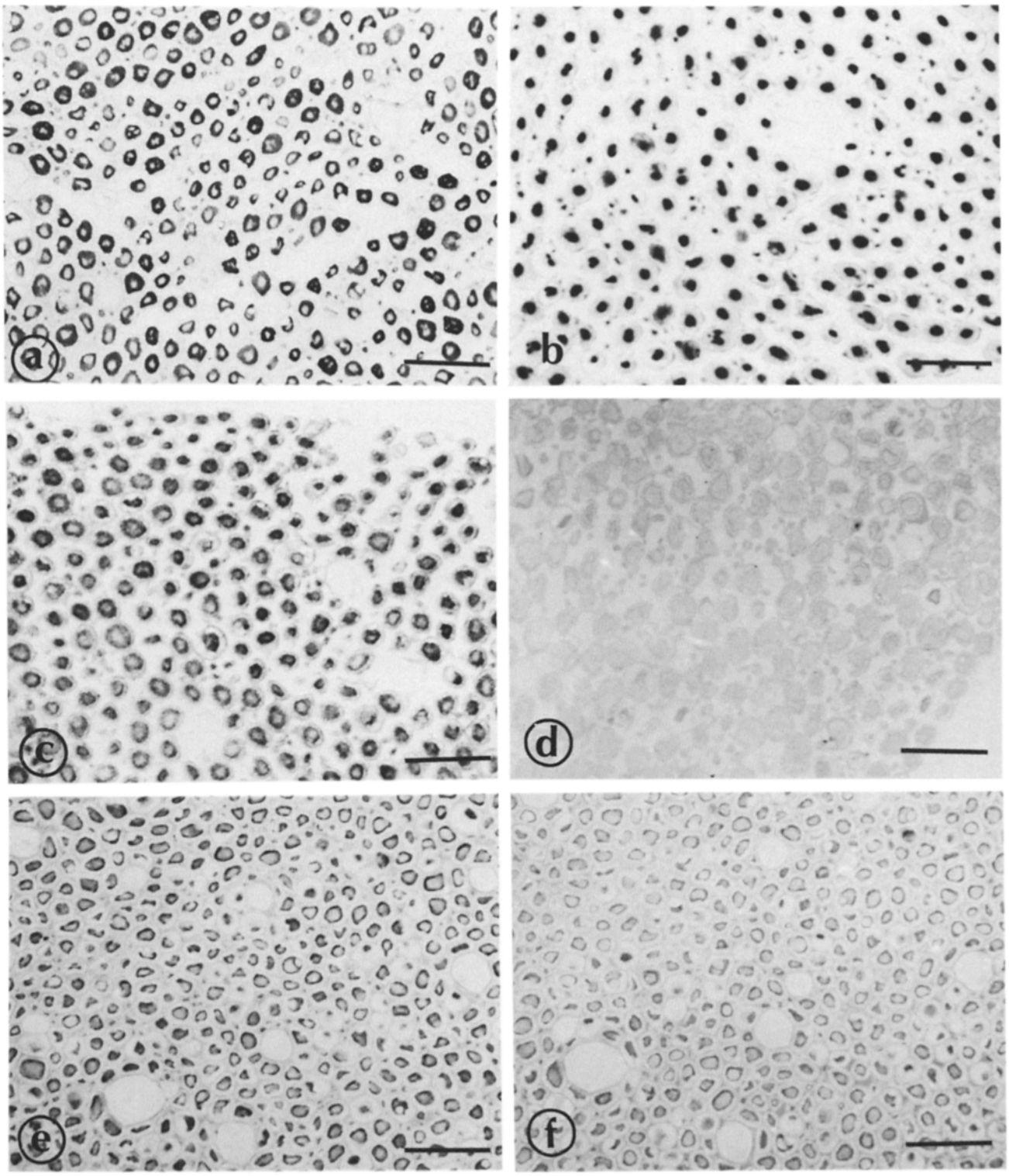

FIGURE 7 Light micrographs of adjacent, Epon-embedded (*a–d*) and serial PEG-embedded sections (*e–f*) of L_5 ventral root, 2 wk after IDPN administration, immunostained with various antibodies. (*a*) Antiserum to 68,000-dalton subunit of neurofilaments, diluted 1:2,000; only the cortical axoplasm is intensely stained; a single or occasionally two or more, smaller, unstained, central areas are present. × 500. (*b*) Affinity-purified, polyclonal antibody against α- and β-tubulin (10 μg/ml). Only the central region of axons is strongly positive and a complementary staining pattern to that obtained with antineurofilament serum is seen. × 500. (c) AP13 (3.9 μg/ml) stained only the cortical axoplasm; it produced a similar staining pattern to that obtained with antineurofilament serum. × 500. (*d*) Adsorption of AP13 on a MAP2 affinity column abolished staining of axons. × 500. (e and *f*) Both the antineurofilament serum (e), diluted 1:1,000, and AP13 (3.9 μg/ml) (*f*), stained only the cortical axoplasm. × 500. None of the above antibodies stained the myelin sheaths, blood vessel walls or connective tissues. Bars, 30 μm.

terminals remained unstained (Fig. 2).

Astrocytes and oligodendrocytes, ependymal, satellite, and Schwann cells were negative for MAP2 immunoreactivity (Figs. 3, *a* and *c*, and 4*b*). Only the astrocytes in the optic nerve and tract were strongly positive (data not shown). The capillary endothelium, pericytes and vascular smooth muscle cells also remained unstained.

In all sections there was no immunoreactivity when absorbed or nonimmune sera were used.

Immunohistochemical Studies of IDPN-treated Spinal Motor Axons

PNS PORTION: IDPN produced reorganization of axoplasmic organelles, with displacement of neurofilaments towards the periphery and of microtubules, smooth endoplasmic reticulum and mitochondria towards the central region of the PNS portion of motor axons. Thus, the antiserum to 68,000-dalton subunit of neurofilaments stained only the peripheral axoplasm, occupied by neurofilaments (Fig. 7, *a* and *e*), and both the affinity-purified, polyclonal antibody to α- and β-tubulin (Fig. 7*b*) and the monoclonal antibody to β-tubulin (Fig. 8) localized only with microtubules in the central region of axons. With the antibodies to tubulin, most of the axons showed a single stained area in the central region, although in a few axons, two or more smaller, separately labeled areas were present. This staining pattern obtained with the antibodies to tubulin was complementary to that obtained with the antineurofilament serum. The above immunoreactivity patterns, demonstrating segregation of microtubules from neurofilaments were observed along the entire length of the sciatic nerve. It is worth noting here that, in IDPN-treated axons, both α- and β-tubulin and the 68,000-dalton subunit of neurofilaments are found only where microtubules and neurofilaments are present, respectively, and not diffusely over the entire cross-section of the axons.

In IDPN-treated motor axons, different localizations were observed with the two antibodies against MAP2; while AP9 localized with microtubules in the central region of axons (Fig. 9*b*), which were frequently surrounding membranous organelles, AP13 localized with neurofilaments at the cortical axoplasm and no staining of microtubules was obtained (Figs. 7*c* and *f*, and 9*c*). To rule out the possibility of nonspecific binding of AP13 to aggregated neurofilaments, sections were treated with alkaline (pH 9.5) Tris-buffered saline, following incubation with AP13, but no diminution in the staining intensity was observed (53). In addition, pre-adsorption of AP13 on a MAP2 affinity column, performed as is described under Materials and Methods, abolished staining of axons (Fig. 7*d*).

CNS PORTION: The CNS portion of a spinal motor axon is the segment of the axon whose myelin sheath is formed by oligodendrocytes, in contrast to Schwann cells in the PNS portion, and is included in the blood-brain barrier. It usually projects for a very short distance into the ventral root, as is well illustrated in Figs. 2*a* and 10*b*. This portion of IDPN-treated motor axons was dilated, tortuous and filled with an increased number of neurofilaments (Figs. 10*a* and 11). There was no apparent accumulation of microtubules, which were spread over the entire cross-section of the axon, and no segregation of microtubules from neurofilaments was present (Fig. 11). In cross and longitudinal sections of this portion of IDPN axons, both antibodies to MAP2 co-localized with microtubules, while neurofilaments remained unstained (Figs. 10*b* and 11).

DISCUSSION

The presence or absence of MAP2 in axons is a controversial issue. Biochemical studies demonstrated significant quantities

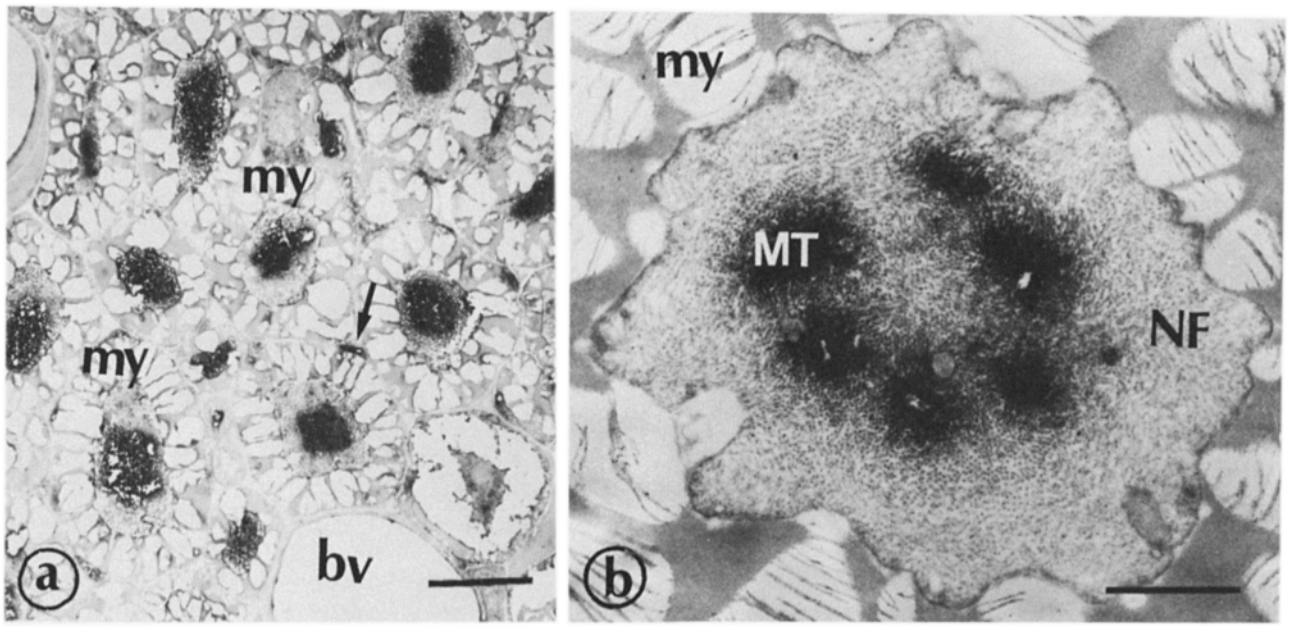

FIGURE 8 Electron micrographs of PEG-embedded (*a*) and vibratome (*b*) sections of L_5 ventral root, 2 wk after IDPN administration. Both sections were immunostained with the monoclonal antibody against β-tubulin (1 μg/ml in *a* and 0.39 μg/ml in *b*). In *a*, only the central region of axons, occupied by microtubules is strongly positive, while the cortical axoplasm, occupied by neurofilaments, remained unstained. The Schwann cell cytoplasm (arrow) is also positive. × 2,730. In *b*, six small groups of microtubules (*MT*) in the central region of this axon are intensely stained, while the segregated neurofilaments (*NF*) are negative. × 18,050. Bars: (*a*) 5 μm; (*b*) 1 μm.

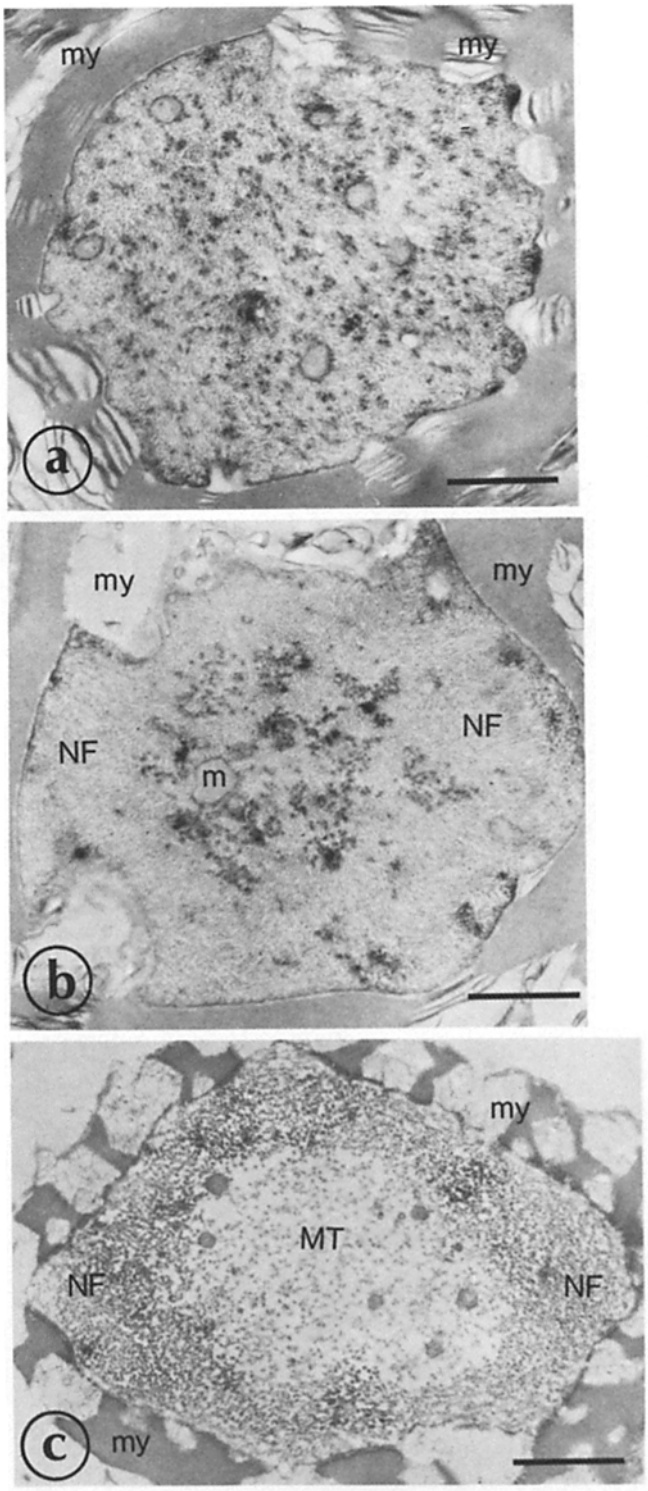

FIGURE 9 Electron micrographs of vibratome sections (a and *b*), immunostained with AP9 (1.5 μg/ml), and PEG-embedded section (*c*) immunostained with AP13 (0.74 μg/ml). *my*, myelin sheath; *m*, mitochondria. (a) L_5 ventral root of a control rat. Only microtubules, that are distributed over the entire cross section of this myelinated axon, are stained. × 15,200. (*b*) L_5 ventral root, 4 d following IDPN administration. Only microtubules, which are mostly found at the central region of the axon, are decorated; neurofilaments (*NF*) are negative. × 15,200. (*c*) L_5 ventral root, 2 wk after IDPN administration. AP13 localized with segregated neurofilaments (*NF*) at the periphery of this myelinated axon, while microtubules (*MT*), mitochondria, and profiles of smooth endoplasmic reticulum are unstained. × 15,200. Bars, 1 μm.

of MAP2 in microtubules purified from bovine white matter tracts (31), however, a number of immunocytochemical studies do not support this finding (25–28). In a recent report, in which the same monoclonal antibodies employed in our present study were used, MAP2 immunoreactivity has been demonstrated in certain CNS axonal tracts (30). In agreement with these findings, we have found MAP2 immunoreactivity in some, but not all axons that we examined.

Monoclonal antibodies are exquisitely specific probes which recognize discrete binding domains on proteins. Should their conjugate epitopes be in some way altered or masked, little or no reaction will be observed. Therefore, a negative immunostaining reaction does not necessarily prove the absence of the target polypeptide. By extension, should the same epitope be present on a polypeptide other than the immunogen, the monoclonal antibody will not distinguish between the two proteins and false positives are possible. In fact, unexpected cross-reactivities with monoclonal antibodies have been reported (54–57). Our monoclonal antibodies bind to only the MAP2 doublet when assayed by either nitrocellulose blotting procedures of whole spinal cord extracts (Fig. 1) or immunoprecipitation of whole brain extracts (Black, M. M., and L. I. Binder, in preparation). By these criteria, they are "monospecific." However, the caveat that axonal staining could represent cross-reactivity with a non-MAP2 species can not be ruled out, although the localization of the anti-MAP2 antibodies with microtubules at the electron microscope level renders this possibility very unlikely.

Therefore, differential staining of various axonal populations by AP9 and AP13 indicates that either (*a*) MAP2 is present in some axons but not in others or, (*b*) different types of axons contain different forms of MAP2. Different forms of MAP2 could be defined by a masking of specific epitopes due to interactions with other axonal proteins or by the modification of the epitope, e.g., by phosphorylation (58), rendering it incapable of antibody binding. Our current results do not distinguish between these possibilities. Differential axonal staining using the anti-MAP2 antibodies was especially evident when the strong immunoreactivity in motor axons of ventral root was compared with the lack of staining in sensory axons in dorsal root and in the white matter tracts of spinal cord. It became also apparent when the peripheral and central processes of the dorsal root ganglion cells were examined. The peripheral processes, which project into the spinal nerves and resemble axons both physiologically and morphologically, but function as dendrites in that they receive information, exhibited strong immunoreaction. In contrast, the central processes which form the dorsal root and not only resemble axons but also function as axons showed no staining. This staining pattern resembles that seen in CNS neurons in which the axons either lack MAP2 immunoreactivity or exhibit only light staining, while the dendrites are heavily stained. In addition, the fact that the dorsal root ganglion cells constitute a heterogeneous cell population (59–63) has also been amply demonstrated in our study by using anti-MAP2 antibodies.

In our model of acute administration of IDPN, neurofilaments accumulate in the CNS portion of spinal motor axons, since their synthesis in the neuronal perikarya and export into the axon continues unimpaired (64), while they can not be transported beyond the CNS-PNS junction. Microtubules do not accumulate to any appreciable extent and previous work indicates that any impediment to the transport of tubulin is secondary to the marked accumulation of neurofilaments (32,

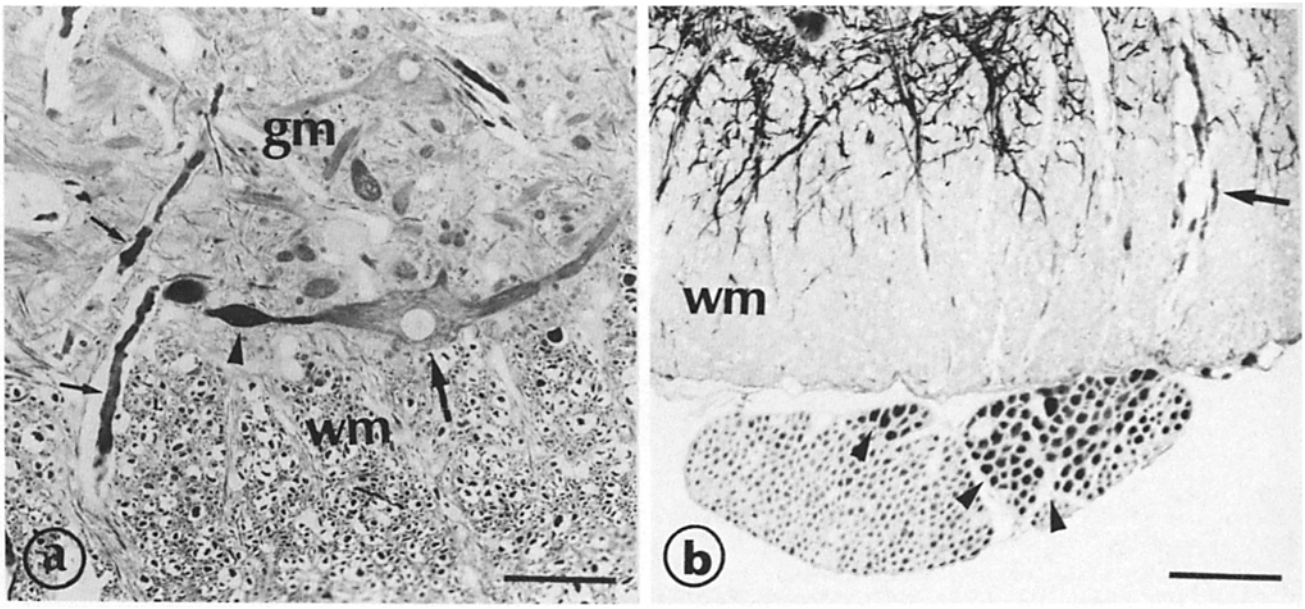

FIGURE 10 (*a*) Epon-embedded section of L_5 segment of spinal cord, 2 wk after IDPN administration, immunostained with the antiserum against the 68,000-dalton subunit of neurofilaments, diluted 1:1,000. *gm*, gray matter; *wm*, white matter. The CNS portions of motor axons are enlarged, tortuous and intensely stained (small arrows). The big arrow points to a motor neuron with weak cytoplasmic and dendritic staining and intense staining of its axon; an early axonal swelling (arrowhead) has appeared. Note how abruptly the staining intensity increases just after the axon hillock. Axons of white matter tracts are strongly positive. Bar, 60 μm. × 250. (*b*) Paraffin-embedded section of lumbar spinal cord and ventral root, 1 wk after IDPN administration. AP9 (1.5 μg/ml) stained strongly both the dilated CNS portion (arrow), which outpouches into the ventral root, and PNS portion of motor axons. The arrowheads delineate the CNS-PNS junction. Bar, 120 μm. × 125.

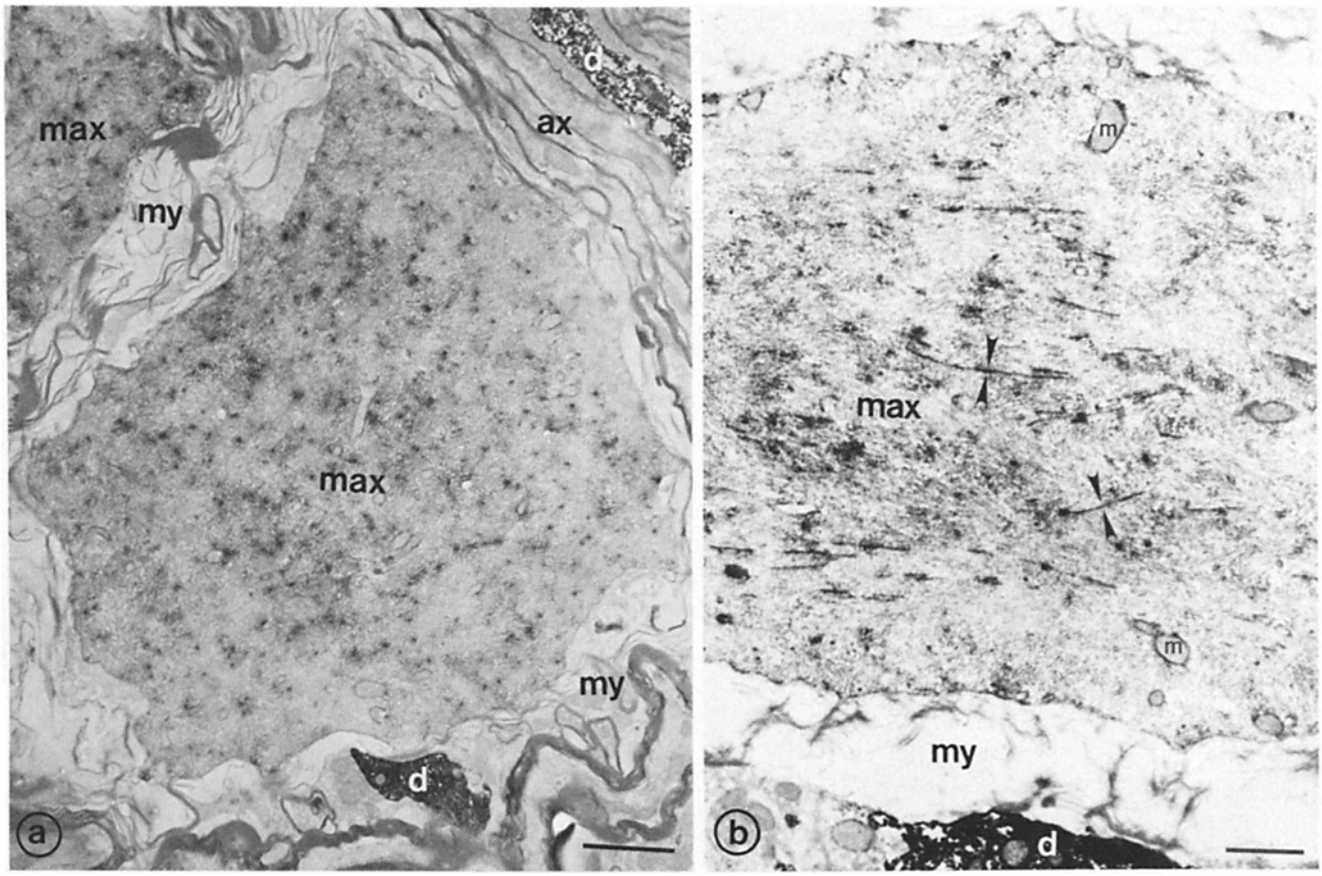

FIGURE 11 Electron micrographs of vibratome sections of the dilated CNS portion of motor axons (*max*), immunostained with AP9 (0.74 μg/ml) in *a* and AP13 (0.78 μg/ml) in *b*. Both AP9 and AP13 localized with microtubules in cross (*a*) and longitudinal sections (between arrowheads in *b*). Mitochondria (*m*) and other membranous organelles are not stained. While nearby dendrites (*d*) are intensely positive, myelinated axons (*ax*) of white matter tracts are negative. Sections were not counterstained with heavy metals. *my*, myelin sheath. Bars: (*a*) 2 μm; (*b*) 1 μm. (*a*) × 6,230; (*b*) × 10,880.

33). Since segregated neurofilaments have MAP2 associated with them in the PNS portion of IDPN-treated axons, one would expect MAP2 to accumulate with the neurofilaments on the CNS side of the CNS-PNS junction, if the association of MAP2 with neurofilaments was independent of microtubules. Our immunocytochemical data indicate that MAP2 does not accumulate but rather is present in apparently normal amounts in proportion to the number of microtubules observed. These findings show that MAP2 is associated with microtubules and is transported down the axons past the CNS-PNS junction. However, MAP2 associated with microtubules in the PNS portion is qualitatively different from that in the CNS portion of motor axons, since it has available only the AP9 epitope whereas, MAP2 on the CNS side will bind both AP9 and AP13.

The localization of MAP2 with segregated neurofilaments in the PNS portion of motor axons is reminiscent of the study by Bloom and Vallee (11), who have found that in cultured brain cells, following depolymerization of microtubules, MAP2 co-localizes with cables of vimentin filaments. In our study, only AP9 stained microtubules in the PNS portion of spinal motor axon after IDPN administration, while AP13 localized with neurofilaments. The reason for this is intriguing, because AP9 and AP13 bind different epitopes on the MAP2 molecule (48). The segregation of these epitopes by IDPN treatment can be explained by several hypotheses. The most straight forward interpretation involves the cleavage (presumably by a protease) of the MAP2 molecule between these epitopes. This hypothesis presupposes that one end of the MAP2 molecule interacts with neurofilaments while the opposite end associates with microtubules. The possibility that IDPN induces a biochemical rather than a structural alteration of the MAP2 molecule should also be considered. While phosphorylation of MAP2 enhances its affinity to neurofilaments (13, 65), it inhibits its interactions with microtubules (66, 67), actin filaments (15, 16, 18), and secretory granules (6, 7). In addition, a recent report showed that axonal neurofilaments become progressively phosphorylated as they are transported away from the cell body (58). Whether the states of phosphorylation of MAP2 and neurofilament proteins define the stability of interactions with each other and with other organelles, and if IDPN interferes with the phosphorylation process of these polypeptides remains to be seen. In this context, it is worth noting the relative immunity of the CNS portion of motor axons to IDPN. Whether this is due to a different composition or organization of their cytoskeleton or to a slower rate of accessibility of IDPN, because of the presence of blood-brain barrier, could not yet be answered. However, all of these theoretical considerations are highly speculative and elucidation of the mechanisms involved in differential MAP2 sequestration by IDPN requires more experimentation.

We thank N. John for typing the manuscript.

This work was supported by a National Institutes of Health grant NS19351 and a Biomedical Research Support Award RR05431 to S. Ch. Papasozomenos.

Received for publication 5 December 1983, and in revised form 15 September 1984.

REFERENCES

1. Kim, H., L. I. Binder, and J. L. Rosenbaum. 1979. The periodic association of MAP2 with brain microtubules in vitro. *J. Cell Biol.* 80:266–276.
2. Sloboda, R. D., S. A. Rudolph, J. L. Rosenbaum, and P. Greengard. 1975. Cyclic AMP-dependent endogenous phosphorylation of a microtubule-associated protein. *Proc. Natl. Acad. Sci. USA.* 72:177–181.
3. Vallee, R. B. 1984. MAP2 (microtubule-associated protein 2). *In* Cell and Muscle Motility. J. W. Shay, editor. Plenum Publishing Corporation, New York. 5:289–311.
4. Smith, D. S. 1971. On the significance of cross-bridges between microtubules and synaptic vesides. *Philos. Trans. R. Soc. Lond. B Biol. Sci.* 261:395–405.
5. Raine, C. S., B. Ghetti, and M. L. Shelanski. 1971. On the association between microtubules and mitochondria within axons. *Brain Res.* 34:389–393.
6. Sherline, P., Y. C. Lee, and L. S. Jacobs. 1977. Binding of microtubules to pituitary secretory granules and secretory granule membranes. *J. Cell Biol.* 72:164–174.
7. Suprenant, K. A., and W. L. Dentler. 1982. Association between endocrine pancreatic secretory granules and in-vitro-assembled microtubules is dependent upon microtubule-associated proteins. *J. Cell Biol.* 93:164–174.
8. Hirokawa, N. 1982. Cross-linker system between neurofilaments, microtubules and membranous organelles in frog axons revealed by quick-freeze, deep-etching method. *J. Cell Biol.* 94:129–142.
9. Schnapp, B. J., and T. S. Reese. 1982. Cytoplasmic structure in rapid-frozen axons. *J. Cell Biol.* 94:667–679.
10. Rice, R. V., P. F. Roslansky, N. Pascoe, and S. F. Houghton. 1980. Bridges between microtubules and neurofilaments visualized by stereoelectron microscopy. *J. Ultrastruct. Res.* 71:303–310.
11. Bloom G. S., and R. B. Vallee. 1983. Association of microtubule-associated protein 2 (MAP2) with microtubules and intermediate filaments in cultured brain cells. *J. Cell Biol.* 96:1523–1531.
12. Berkowitz, S. A., J. Katagiri, H.-K. Binder, and R. C. Williams, Jr. 1977. Separation and characterization of microtubule proteins from calf brain. *Biochemistry.* 16:5610–5617.
13. Runge, M. S., T. M. Laue, D. A. Yphantis, M. R. Lifsics, A. Saito, M. Altin, K. Reinke, and R. C. Williams, Jr. 1981. ATP-induced formation of an associated complex between microtubules and neurofilaments. *Proc. Natl. Acad. Sci. USA.* 78:1431–1435.
14. Leterrier, J.-F., R. K. H. Liem, and M. L. Shelanski. 1982. Interactions between neurofilaments and microtubule-associated proteins: a possible mechanism for intraorganellar bridging. *J. Cell Biol.* 95:982–986.
15. Sattilaro, W., L. Dentler, and E. L. LeCluyse. 1981. Microtubule-associated proteins (MAPs) and the organization of actin filaments in vitro. *J. Cell Biol.* 90:467–473.
16. Nishida, E., T. Kuwaki, and H. Sakai. 1981. Phosphorylation of microtubule-associated proteins (MAPs) and pH of the medium control interaction between MAPs and actin filaments. *J. Biochem.* 90:575–578.
17. Griffith, L., and T. D. Pollard. 1982. The interaction of actin filaments with microtubules and microtubule-associated proteins. *J. Biol. Chem.* 257:9143–9151.
18. Selden, S. C., and T. D. Pollard. 1983. Phosphorylation of microtubule-associated proteins regulates their interaction with actin filaments. *J. Biol. Chem.* 258:7064–7071.
19. Izant, J. G., and J. R. McIntosh. 1980. Microtubule-associated proteins: a monoclonal antibody to MAP2 binds to differentiated neurons. *Proc. Natl. Acad. Sci. USA.* 77:4741–4745.
20. Sheterline, P. 1978. Localization of the major high-molecular-weight protein on microtubules in vitro and in cultured cells. *Exp. Cell Res.* 115:460–464.
21. Sloboda, R. D., and K. Dickersin. 1980. Structure and composition of the cytoskeleton of nucleated erythrocytes. I. The presence of microtubule-associated protein 2 in the marginal band. *J. Cell Biol.* 87:170–179.
22. Kuznetsov, S. A., V. I. Rodionov, A. D. Bershadsky, V. I. Gelfand, and V. A. Rosenblat. 1980. High molecular weight protein MAP2 promoting microtubule assembly in vitro is associated with microtubules in cells. *Cell Biol. Int. Rep.* 4:1017–1024.
23. Weatherbee, J. A., P. Sherline, R. N. Mascardo, J. G. Izant, R. B. Luftig, and R. R. Weihing. 1982. Microtubule-associated proteins of HeLa cells: heat stability of the 200,000 molecular weight HeLa MAPs and detection of the presence of MAP2 in HeLa cell extracts and cycled microtubules. *J. Cell Biol.* 92:155–163.
24. Valdivia, M. M., J. Avila, J. Coll, C. Colaco, and I. V. Sandoval. 1982. Quantitation and characterization of the microtubule associated MAP2 in porcine tissues and its isolation from porcine (PK15) and human (HeLa) cell lines. *Biochem. Biophys. Res. Commun.* 105:1241–1249.
25. Matus, A., R. Bernhardt, and T. Hugh-Jones. 1981. High molecular weight microtubule-associated proteins are preferentially associated with dendritic microtubules in brain. *Proc. Natl. Acad. Sci. USA.* 78:3010–3014.
26. Huber, G., and A. Matus. 1984. Differences in the cellular distribution of two microtubule-associated proteins MAP1 and MAP2 in rat brain. *J. Neurosci.* 4:151–160.
27. Wiche, G., E. Briones, H. Hirt, R. Krepler, U. Artlieb, and H. Denk. 1983. Differential distribution of microtubule-associated proteins MAP-1 and MAP-2 in neurons of rat brain and association of MAP-1 with microtubules of neuroblastoma cells (clone N_2A). *EMBO J.* 2:1915–1920.
28. DeCamilli, P., P. E. Miller, F. Navone, W. E. Theurkauf, and R. B. Vallee. 1984. Distribution of microtubule-associated protein 2 in the nervous system of the rat studied by immunofluorescence. *Neuroscience.* 11:819–846.
29. Tytell, M., S. T. Brady, and R. J. Lasek. 1984. Axonal transport of a subclass of tau proteins: Evidence for the regional differentiation of microtubules in neurons. *Proc. Natl. Acad. Sci. USA.* 81:1570–1574.
30. Caceres A., L. I. Binder, M. R. Payne, P. Bender, L. Rebhun, and O. Steward. 1984. Differential subcellular localization of tubulin and the microtubule-associated protein MAP2 in brain tissue as revealed by immunocytochemistry with monoclonal hybridoma antibodies. *J. Neurosci.* 4:394–410.
31. Vallee, R. B. 1982. A taxol-dependent procedure for the isolation of microtubules and microtubule-associated proteins (MAPs). *J. Cell Biol.* 92:435–442.
32. Griffin, J. W., P. N. Hoffman, A. W. Clark, P. T. Carroll, and D. L. Price. 1978. Slow axonal transport of neurofilament proteins: impairment by β,β'-iminodipropionitrile administration. *Science (Wash. DC).* 202:633–635.
33. Yokoyama, K., S. Tsukita, H. Ishikawa, and M. Kurokawa. 1980. Early changes in the neuronal cytoskeleton caused by β,β'-iminodipropionitrile: selective impairment of neurofilament polypeptides. *Biomed. Res.* 1:537–547.
34. Papasozomenos, S. Ch., M. Yoon, R. Crane, L. Autilio-Gambetti, and P. Gambetti. 1982. Redistribution of proteins of fast axonal transport following administration of β,β'-iminodipropionitrile: a quantitative autoradiographic study. *J. Cell Biol.* 95:672–675.
35. Chou, S. M., and H. A. Hartmann. 1964. Axonal lesions and waltzing syndrome after IDPN administration in rats. *Acta Neuropathol.* 3:428–450.
36. Chou, S. M., and H. A. Hartmann. 1965. Electron microscopy of focal neuroaxonal lesions produced by β,β'-iminodipropionitrile (IDPN) in rats. *Acta Neuropathol.* 4:590–603.

37. Papasozomenos, S. Ch., L. Autilio-Gambetti, and P. Gambetti. 1981. Reorganization of axoplasmic organelles following β,β′-iminodipropionitrile administration. *J. Cell Biol.* 91:866–871.
38. Papasozomenos, S. Ch., L. Autilio-Gambetti, and P. Gambetti. 1982. The IDPN axon: rearrangement of axonal cytoskeleton and organelles following β,β′-iminodipropionitrile (IDPN) intoxication. *In* Axoplasmic Transport. D. G. Weiss, editor. Springer-Verlag, Inc., Berlin. 241–250.
39. Griffin, J. W., K. E. Fahnestock, D. L. Price, and P. N. Hoffman. 1983. Microtubule-neurofilament segregation produced by β,β′-iminodipropionitrile: evidence for the association of fast axonal transport with microtubules. J. Neurosci. 3:557–566.
40. Papasozomenos, S. C., L. I. Binder, P. Bender, and M. R. Payne. 1982. A monoclonal antibody to microtubule-associated protein 2 (MAP2) localizes with neurofilaments in the β,β′-iminodipropionitrile (IDPN) model. *J. Cell Biol.* 95:341*a*. (Abstr.)
41. Payne, M. R. 1983. Monoclonal antibodies to the contractile proteins. *In* Cell and Muscle Motility. R. M. Dowben and J. W. Shay, editors. Plenum Publishing Corporation, New York. 4:137–177.
42. Bender, P. K. 1982. Microtubule-associated proteins. Ph.D. Thesis, University of Virginia. pp. 19–45.
43. Laemmli, U. K. 1970. Cleavage of structural proteins during the assembly of the head of bacteriophage T_4. *Nature (Lond).* 227:680–685.
44. Binder, L. I., and J. L. Rosenbaum. 1978. The in vitro assembly of flagellar outer doublet tubulin. *J. Cell Biol.* 79:500–515.
45. Towbin, H., T. Staehelin, and J. Gordon. 1979. Electrophoretic transfer of proteins from polyacrylamide gels to nitrocellulose sheets: procedure and some applications. *Proc. Natl. Acad. Sci. USA.* 76:4350–4354.
46. Sternberger, L. A., P. H. Hardy, J. J. Cuculis, and H. G Meyer. 1970. The unlabeled antibody enzyme method of immunohistochemistry. Preparation and properties of soluble antigen-antibody complex (horseradish peroxidase-antihorseradish peroxidase) and its use in identification of spirochetes. *J. Histochem. Cytochem.* 18:315–333.
47. Straus, W. 1982. Imidazole increases the sensitivity of the cytochemical reaction for peroxidase with diaminobenzidine at a neutral pH. *J. Histochem. Cytochem.* 30:491–493.
48. Binder, L. I., M. R. Payne, H. Kim, V. R. Sheridan, D. K. Schroeder, C. C. Walker, and L. I. Rebhun. 1982. Production and analysis of monoclonal hybridoma antibodies specific for β-tubulin and MAP2. *J. Cell Biol.* 95:349*a*. (Abstr.)
49. Autilio-Gambetti, L., M. E. Velasco, P. Gambetti, and J. Sipple. 1981. Immunochemical characterization of antisera to rat neurofilament subunits. *J. Neurochem.* 37:1260–1265.
50. Smithson, K. G., B. A. MacVicar, and G. I. Hatton. 1983. Polyethylene glycol embedding: a technique compatible with immunocytochemistry, enzyme histochemistry, histofluorescence and intracellular staining. *J. Neurosci. Methods* 7:27–41.
51. Wolosewick, J., and J. DeMey. 1982. Localization of tubulin and actin in polyethylene glycol embedded rat seminiferous epithelium. *Biol. Cell.* 44:85–88.
52. Mayor, D. H., J. C. Hampton, and B. Rosario. 1961. A simple method for removing the resin from epoxy-embedded tissue. *J. Biophys. Biochem. Cytol.* 9:909–910.
53. Bennett, G. S., S. A. Fellini, J. M. Croop, J. J. Otto, J. Bryan, and H. Holtzer. 1978. Differences among 100-A filament subunits from different cell types. *Proc. Natl. Acad. Sci. USA.* 75:4364–4368.
54. Pruss, R. M., R. Mirsky, M. C. Raff, R. Thorpe, A. J. Dowding, and B. H. Anderton. 1981. All classes of intermediate filaments share a common antigenic determinant defined by a monoclonal antibody. *Cell.* 27:4119–4228.
55. Blose, S. H., F. Matsumura, and J. J.-C. Lin. 1981. Structure of vimentin 10-nm filaments probed with a monoclonal antibody that recognizes a common antigenic determinant on vimentin and tropomyosin. *Cold Spring Harbor Symp. Quant. Biol.* 46:455–463.
56. Dulbecco, R., M. Unger, M. Bologna, H. Battifora, P. Syka, and S. Okada. 1981. Cross-reactivity between Thy-1 and a component of intermediate filaments demonstrated using a monoclonal antibody. *Nature (Lond.).* 292:772–774.
57. Nigg, E. A., G. Walter, and S. J. Singer. 1982. On the nature of crossreactions observed with antibodies directed to defined epitopes. *Proc. Natl. Acad. Sci. USA.* 79:5939–5943.
58. Sternberger, L. A., and N. H. Sternberger. 1983. Monoclonal antibodies distinguish phosphorylated and nonphosphorylated forms of neurofilaments in situ. *Proc. Natl. Acad. Sci. USA.* 80:6126–6130.
59. Bunge, M. B., R. P. Bunge, E. R. Peterson, and M. R. Murray. 1967. A light and electron microscope study of long-term organized cultures of rat dorsal root ganglia. *J. Cell Biol.* 32:439–466.
60. Duce, I. R., and P. Keen. 1977. An ultrastructural classification of the neuronal cell bodies of the rat dorsal root ganglion using zinc iodide-osmium impregnation. *Cell Tissue Res.* 185:263–277.
61. Shaw, G., and K. Weber. 1981. The distribution of the neurofilament triplet proteins within individual neurones. *Exp. Cell Res.* 136:119–125.
62. Sharp, G. A., G. Shaw, and K. Weber. 1982. Immunoelectron microscopical localization of the three neurofilament triplet proteins along neurofilaments of cultured dorsal root ganglion neurones. *Exp. Cell Res.* 137:403–413.
63. Dahl, D. 1983. Immunohistochemical differences between neurofilaments in perikarya, dendrites and axons. *Exp. Cell Res.* 149:394–408.
64. Chou, S. M., and R. A. Klein. 1972. Autoradiographic studies of protein turnover in motoneurons of IDPN-treated rats. *Acta. Neuropathol.* 22:183–189.
65. Leterrier, J.-F., R. K. H. Liem, and M. L. Shelanski. 1981. Preferential phosphorylation of the 150,000 molecular weight component of neurofilaments by a cyclic AMP-dependent microtubule-associated protein kinase. *J. Cell Biol.* 90:755–760.
66. Jameson, L., and M. Caplow. 1981. Modification of microtubule steady-state dynamics by phosphorylation of the microtubule-associated proteins. *Proc. Natl. Acad. Sci. USA.* 78:3413–3417.
67. Murthy, A. S. N., and M. Flavin. 1983. Microtubule assembly using the microtubule-associated protein MAP2 prepared in defined states of phosphorylation with protein kinase and phosphatase. *Eur. J. Biochem.* 137:37–46.